Proc. Natl. Acad. Sci. USA
Vol. 86, pp. 7746–7750, October 1989
Biochemistry

Sensory rhodopsins I and II modulate a methylation/demethylation system in *Halobacterium halobium* phototaxis

(archaebacteria/photosensory receptors/retinal proteins/signal transduction/adaptation)

E. N. SPUDICH, T. TAKAHASHI*, AND J. L. SPUDICH

Department of Anatomy and Structural Biology and Department of Physiology and Biophysics, Albert Einstein College of Medicine, Bronx, NY 10461

Communicated by Julius Adler, July 14, 1989

ABSTRACT **This work demonstrates that phototaxis stimuli in the archaebacterium *Halobacterium halobium* control a methylation/demethylation system *in vivo* through photoactivation of sensory rhodopsin I (SR-I) in either its attractant or repellent signaling form as well as through the repellent receptor sensory rhodopsin II (SR-II, also called phoborhodopsin). The effects of positive stimuli that suppress swimming reversals (i.e., an increase in attractant or decrease in repellent light) and negative stimuli that induce swimming reversals (i.e., a decrease in attractant or increase in repellent light) through each photoreceptor were monitored by assaying release of volatile [^{3}H]methyl groups. This assay has been used to measure [^{3}H]methanol produced during the process of adaptation to chemotactic stimuli in eubacteria. In *H. halobium* positive photostimuli produce a transient increase in the rate of demethylation followed by a decrease below the unstimulated value, whereas negative photostimuli cause an increase followed by a rate similar to that of the unstimulated value. Photoactivation of the SR-I attractant and simultaneous photoactivation of the SR-II repellent receptors cancel in their effects on demethylation, demonstrating the methylation system is regulated by an integrated signal. Analysis of mutants indicates that the source for the volatile methyl groups is intrinsic membrane proteins distinct from the chromoproteins that share the membrane. A methyl-accepting protein (94 kDa) previously correlated in amount with the SR-I chromoprotein (25 kDa) is shown here to be missing in a recently isolated SR-I$^-$SR-II$^+$ mutant (Flx3b), thus confirming the association of this protein with SR-I. Photoactivated SR-II in mutant Flx3b controls demethylation, predicting the existence of a photomodulated methyl-accepting component distinct from the 94-kDa protein of SR-I. We present a model in which the three known phototaxis signaling receptor states (the attractant receptor SR-I$_{587}$, its repellent form S$_{373}$, and the repellent receptor SR-II$_{490}$) are coupled to two distinct transducers the demethylation of which is controlled by one integrated signal.**

Phototactic behavior by the archaebacterium *Halobacterium halobium* is mediated by two retinal-containing chromoproteins, sensory rhodopsins I and II [SR-I and SR-II (also called phoborhodopsin or P480); for reviews, see refs. 1 and 2]. The photosensory system of this primitive organism detects changes in light intensity and color and enables the cells to accumulate in yellow–red regions of the spectrum (attractant light) and to avoid potentially damaging UV–blue repellent light (3). SR-I exists in two photoconvertible forms: one absorbs maximally at 587 nm and is an attractant receptor; the other, a long-lived photoproduct of SR-I that absorbs in the near-UV (species S$_{373}$), is a repellent receptor (4–6). The presence of an additional repellent receptor was strongly suggested by repellent action at wavelengths longer than those absorbed by S$_{373}$ (7–11), and the pigment was first detected and characterized spectroscopically by flash photolysis (8, 12). SR-II absorbs light in the midvisible region [λ_{max} 490 nm (2)]. Study of the sensory rhodopsins has been facilitated by isolation of *H. halobium* mutants lacking the related light-driven ion pumps bacteriorhodopsin (BR) and halorhodopsin (HR) [Flx mutants (13)]. HR and BR absorb in the spectral region where the two sensory rhodopsins are active, interfering with spectroscopic measurements. Moreover, photoactivated BR and HR generate transmembrane electrical potential, which influences sensory rhodopsin photocycling rates (14) and phototaxis behavior (15).

A clue to the mechanism of information transfer from the SR-I chromophoric protein was the finding of a methyl-accepting protein of ≈94 kDa covariant in a series of mutants with the SR-I chromophoric protein of 25 kDa (16). The 94-kDa protein resembles the chemotaxis signal generators ("transducers") of eubacteria (e.g., *Escherichia coli*), which transmit chemoreceptor signals from the membrane to a cytoplasmic sensory pathway. In eubacteria methylation of the transducers occurs by carboxylmethyl esterification of glutamate residues in the signal-transmitting domain and mediates adaptation to chemostimuli (17–20).

Reversible protein methylation was implicated in phototaxis and chemotaxis adaptation in *H. halobium* before the identification of specific taxis receptors (21–25). Methyl-accepting membrane proteins in the 90- to 150-kDa range can be visualized by autofluorography of protein gels and are lost in taxis$^-$ mutants (16, 26), are regained upon reversion to taxis$^+$ (16), and exhibit changes in extent of methylation induced by chemostimuli (26). The lability of the methyl linkages to mild base indicates these proteins are carboxylmethylated (16, 26). Hydrolysis of the carboxylmethyl ester bonds in *E. coli* results in methanol production (27, 28), which has been used to monitor methylesterase activity *in vivo* (29) and to detect changes in the rate of carboxylmethyl hydrolysis induced by chemostimuli (30). Applying this assay to *H. halobium*, Alam *et al.* (26) observed increases in the rate of evolution of volatile methyl groups after stimulation with chemotaxis effectors. Light-induced increases were also reported (26). These observations provided evidence for methylation involvement in phototaxis, but demonstration of control of methylation by photoactivation of the known photoreceptors was not available.

Computerized cell-tracking methods have been implemented to study swimming behavior of *H. halobium* in response to selective photoactivation of SR-I and SR-II (31, 32), and spectroscopic procedures have been developed to monitor SR-I and SR-II photochemical reactions (5, 8–10, 12). In the work presented here, we have applied these methods to characterize receptor mutants and to investigate

The publication costs of this article were defrayed in part by page charge payment. This article must therefore be hereby marked "*advertisement*" in accordance with 18 U.S.C. §1734 solely to indicate this fact.

Abbreviations: SR-I and -II, sensory rhodopsin I and II, respectively; BR, bacteriorhodopsin; HR, halorhodopsin.

*On leave from Department of Pharmaceutical Sciences, Hokkaido University, Sapporo 060 Japan.

the relationship of the *H. halobium* methylation system to photoactivation of the signaling states of SR-I and SR-II.

MATERIALS AND METHODS

Mutant Lineage and Culture Conditions. All strains used are BR^-HR^- (Flx mutants) derived from *H. halobium* strain OD2 (13). Flx3 and Flx15 are $SR\text{-}I^+SR\text{-}II^+$ (10, 32). Flx3b was isolated from Flx3 and is $SR\text{-}I^-SR\text{-}II^+$ (2). Pho81 was selected from Flx15 as blind to white light and chemotaxis-competent (33) and is $SR\text{-}I^-SR\text{-}II^-$ (10). Flx5R is a retinal-deficient mutant that produces relatively large amounts of SR-I apoprotein and no detectable SR-II apoprotein (10). Cultures were grown to early stationary phase as described (13), except to obtain retinal-deficient membranes from Flx3b, cultures were grown with vigorous aeration and harvested in exponential phase ($2–5 \times 10^8$ cells per ml) where retinal production is minimal.

Behavioral Assays. Cell behavior was monitored with nonactinic infrared illumination [>700 nm (4)]. Swimming-response video data were acquired and analyzed with a computerized cell-tracking system, as described (32). Light stimuli were as described in ref. 32, except a 390-nm stimulus was used at 2×10^5 ergs·cm^{-2}·sec^{-1} instead of the 400-nm stimulus. All optical filters for the behavioral measurements were as described below.

[^{3}H]Retinal-Labeling of Membranes. All-*trans*-[^{3}H]retinal was purified from a mixture of [^{3}H]retinal isomers by HPLC [normal-phase silica, semipreparative 5-μm pore column, 8% (wt/vol) ethyl acetate in hexane]. Photoreceptor activities were monitored by absorption and flash spectroscopy during all-*trans*-[^{3}H]retinal reconstitution, and $NaCNBH_3$ reduction of the pigments in sonicated membrane vesicles (10). Labeled proteins were visualized by SDS/PAGE and autofluorography (10).

***In Vivo* [^{3}H]Methyl Labeling.** Labeling with L-[*methyl*-^{3}H]-methionine and processing of membrane proteins for autofluorography were as described (16). The flow assay for volatile [^{3}H]methyl production was essentially as described by Kehry *et al.* (29, 30) with the modifications introduced by Alam *et al.* (26). Samples of 0.5 ml were sequentially collected at a flow rate of 1.25 ml/min into 1.5-ml microcentrifuge tubes, which at the end of the collection were transferred to 20-ml scintillation vials containing 7 ml of Aquasol (New England Nuclear). The vials were incubated 18–20 hr at 23° to allow volatile radioactivity to be transferred via vapor phase to the scintillation fluid (34). The void volume of the filter and outlet tubing is 0.4 ml. Data are shown after the initial 12 min of continuous flow.

Light from a 12-V 100-W tungsten-halogen lamp was passed through 4-mm heat-absorbing glass (Edmund Scientific, Barrington, NJ) and a 600 ± 20 nm (for $SR\text{-}I_{587}$ stimuli) or 450 ± 20 nm (for $SR\text{-}II_{490}$ stimuli) interference filter and through a focusing lens to produce a uniform spot equal to the area of the acrodisc filter. Intensities of 600-nm and 450-nm light were 6.3×10^5 or 6.6×10^4 ergs·cm^{-2}·sec^{-1}, respectively, at the acrodisc filter surface. These photostimuli were saturating. In Fig. 6, the 450-nm light was 1.6×10^5 ergs·cm^{-2}·sec^{-1} from a 200-W mercury arc lamp beam delivered at a 45° angle to the acrodisc filter, and the 600-nm light was as above. The same geometry was used for the 390-nm stimulus (mercury lamp output filtered through a 400 ± 20-nm bandpass filter and a Corning 7-59 shortpass filter to produce 6.0×10^4 ergs·cm^{-2}·sec^{-1}). All optical filters were from Ditric Optics (Hudson, MA), except the 400-nm bandpass, which was from Corion (Holliston, MA).

RESULTS AND DISCUSSION

Mutant Strains Exhibit Selective Loss of SR-I or SR-II Phototaxis Responses. Flx15 and Pho81 have the phenotypes $SR\text{-}I^+SR\text{-}II^+$ and $SR\text{-}I^-SR\text{-}II^-$, respectively (10, 33) and exhibit membrane protein carboxylmethylation (16, 26). Their behavioral responses to light stimuli designed to selectively activate SR-I and SR-II are shown by motion analysis (Fig. 1). The abrupt step-down in 600-nm light (Fig. 1 *Left*) causes a sudden decrease in photoexcitation of $SR\text{-}I_{587}$, the attractant receptor form of SR-I. Flx15 cells react to this negative stimulus by a transient increase in reversal frequency (Fig. 1). The step-up in 390-nm light in a 600-nm background photoactivates S_{373}, the repellent form of SR-I (Fig. 1 *Center*, Flx15). The step-up in 450-nm light photoactivates SR-II (Fig. 1 *Right*, Flx15 and Flx3b). SR-I responses are missing in strain Flx3b (Fig. 1), confirming the $SR\text{-}I^-SR\text{-}II^+$ phenotype reported by Takahashi *et al.* (2). The lack of responses by Pho81 to all of these stimuli is consistent with the absence of both photoreceptors according to flash spectroscopy (10, 33). In all the cases in Fig. 1 in which reversal induction is caused by a change in light intensity, a change in the opposite direction suppresses reversals (data not shown). In unstimulated conditions, the mean time between reversals ± SD for >100 intervals from 30–50 indi-

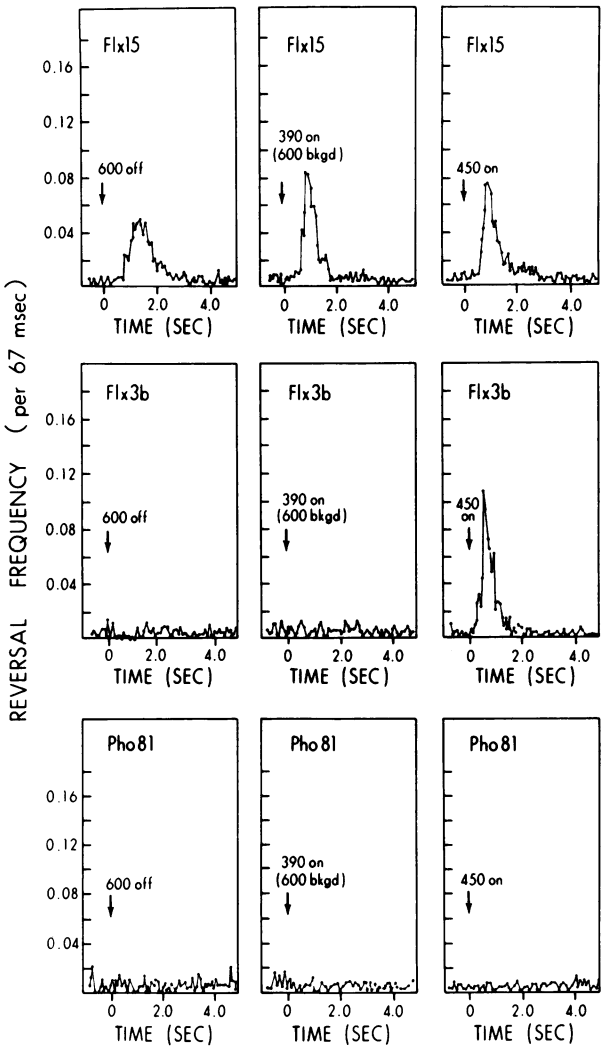

FIG. 1. Reversal frequency responses to photostimuli. Video data were processed with a computerized motion-analysis system (32) at 15 frames per sec, and population reversal frequencies (number of reversals occurring within the 67-msec frame interval per number of paths present in that interval) were determined. Approximately 1000 paths are used for the calculation of each frequency plot. At the arrows, a constant 600-nm light was interrupted for 2 sec (*Left*), a 390-nm light was delivered for 2 sec in a constant 600-nm background (*Center*), or a 450-nm light was delivered for 2 sec (*Right*). Phenotypes: Flx15, $SR\text{-}I^+SR\text{-}II^+$; Flx3b, $SR\text{-}I^-SR\text{-}II^+$; Pho81, $SR\text{-}I^-SR\text{-}II^-$.

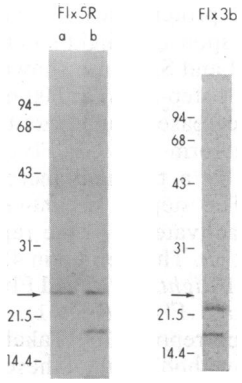

FIG. 2. Autofluorograms of [^{3}H]retinal-labeled proteins. All-*trans*-[^{3}H]retinal was added to Flx5R vesicles at molar ratios [^{3}H]retinal:SR-I apoprotein of 1:1 (lane a) or 3:1 (lane b), and to retinal-deficient Flx3b vesicles at a molar ratio [^{3}H]retinal:SR-II apoprotein of 3:1. Retinal addition reconstituted only SR-I in Flx5R and only SR-II in Flx3b, as determined by absorption spectroscopy. Proteins were electrophoretically separated on an SDS/12% polyacrylamide gel. The 25-kDa band in Flx5R (arrow) in lane a was run as a marker in a lane adjacent to the Flx3b lane, and its position in that gel is marked by the arrow. (This marker and the molecular mass standards were run in each of the two gels from which autofluorographic data are shown.) Standards (Bio-Rad) from top to bottom are ($\times 10^3$ kDa): phosphorylase b, bovine serum albumin, ovalbumin, carbonic anhydrase, soybean trypsin inhibitor, and lysozyme.

vidually tracked cells of each strain was 28 ± 5 sec, 22 ± 5 sec, and 27 ± 5 sec for Flx15, Flx3b, and Pho81, respectively.

The Two Known SR-I Proteins Are Missing in Flx3b. Two proteins have been identified as associated with SR-I function: a 25-kDa chromophoric protein (10, 35) and a 94-kDa methyl-accepting protein (16). Membrane proteins from Flx5R that contains SR-I only exhibit a single band corresponding to the SR-I chromophoric protein when labeled with subsaturating amounts of all-*trans*-[^{3}H]retinal (Fig. 2, lane a). Excess [^{3}H]retinal labels an additional band at 19 kDa and shows light labeling at 94 kDa (Fig. 2, lane b). These latter two retinal binding sites do not appear to generate any absorbing or photocycling pigments (refs. 10 and 16 and unpublished work). In Flx3b membranes, labeled with excess retinal, a 23-kDa band is evident that is not present in Flx5R and previously has been attributed to the SR-II chromophoric protein (10). Thus, the properties of Flx3b confirm the assignments of the 23-kDa retinal-labeled band to SR-II and the 25-kDa retinal-labeled band to SR-I (10, 16).

Membrane proteins from cells labeled *in vivo* with L-[*methyl*-^{3}H]methionine were separated by SDS/PAGE and examined by autofluorography. The arrow marks the position of the 94-kDa protein in Flx5R (Fig. 3). This labeled band is missing in Flx3b as well as in Pho81 (Fig. 3) and is present in their respective parents Flx3 and Flx15 (ref. 16 and unpublished work), confirming its association with SR-I. The other bands have been implicated in chemotaxis by mutant and revertant analysis (16), and some have been shown to exhibit changes in their extent of methyl-labeling after chemotaxis stimuli (26).

SR-I in Both Its Attractant and Repellent Forms and SR-II Modulate Demethylation. Photostimulation of the SR-I attractant form in Flx15 cells produces a transient increase in the release of volatile [^{3}H]methyl groups (600-nm light, Fig. 4). When this light is abruptly decreased, a larger release of

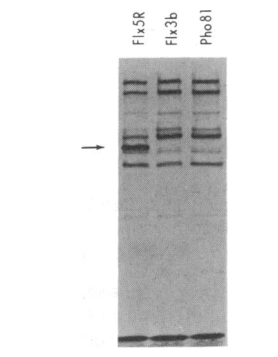

FIG. 3. Autofluorogram of [^{3}H]methylated membrane proteins. Cells were labeled *in vivo* with L-[*methyl*-^{3}H]methionine (75–80 Ci/mmol; 1 Ci = 37 GBq) in the presence of puromycin, and their membrane proteins were electrophoretically separated on a low bisacrylamide/SDS gel as described (16). Arrow, the position of the 94-kDa methyl-accepting protein (see text).

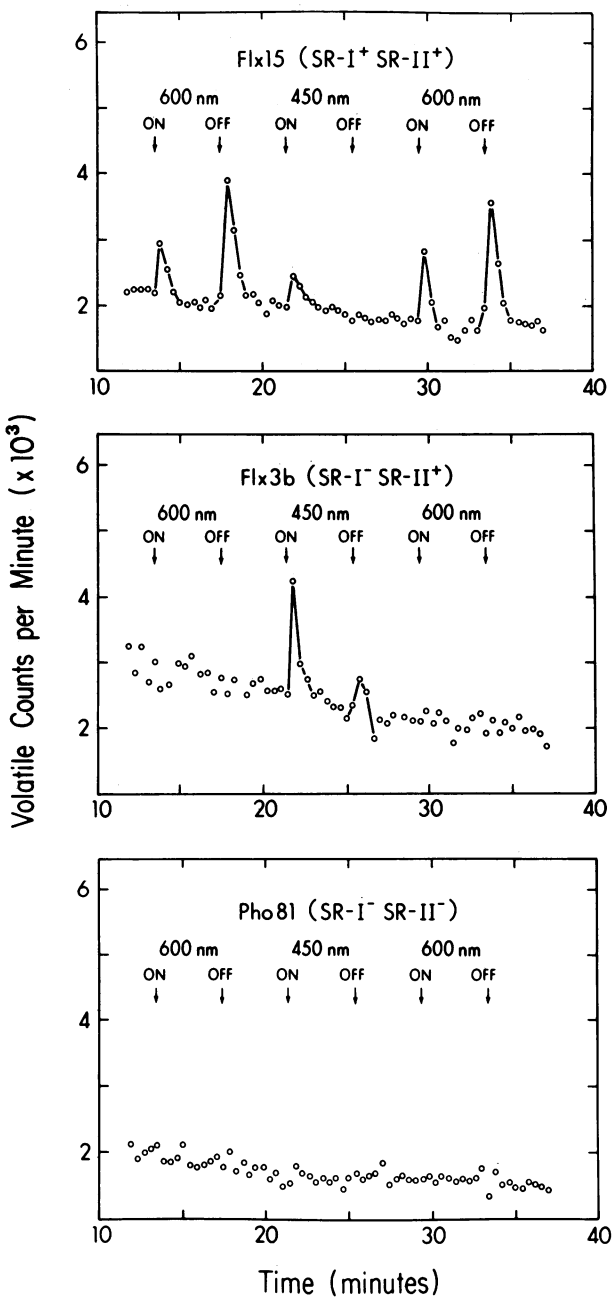

FIG. 4. Volatile [^{3}H]methyl release after photostimulation of the three strains of Fig. 1. Each point corresponds to volatile cpm contained in a 0.5-ml (24 sec) fraction. Buffer was pumped at 1.25 ml/min through the filter apparatus containing cells radiolabeled as in Fig. 3. The continuously flowing buffer contained 200× excess unlabeled methionine.

volatile [^{3}H]methyl occurs. This same stimulus does not cause a response in Flx3b or Pho81, showing the effect is due to SR-I photoactivation. A small response is seen in Flx15 to 450-nm light, which photoactivates SR-II. SR-II photoactivation modulates [^{3}H]methyl evolution because Flx3b is lacking SR-I and exhibits a pronounced response to this stimulus (Fig. 4). No response is seen in Pho81, which lacks both receptors.

An asymmetry in the response is observed in that for each receptor, the reversal-inducing step change in intensity (for SR-I, the step-down, and for SR-II, the step-up) has a greater effect than the reversal-suppressing step change (Fig. 4).

Unlike in *E. coli*, where transient increases and decreases in methanol evolution rate occur in response to negative and positive chemical stimuli, respectively (30), in *H. halobium* both positive (reversal-suppressing) and negative (reversal-inducing) stimuli elicit a transient increase in the rate of volatile methyl evolution. Increases have been reported for other positive and negative stimuli in *H. halobium* (26) and in *Bacillus subtilis* (36). The decrease in baseline is expected from the cold methionine chase in the continuously flowing buffer (29). Relative to this baseline, a period of reduced methyl-release rate occurs after positive stimulus peaks, whereas negative stimulus peaks are followed by a rate equal to or higher than the baseline (e.g., 600 nm on vs. off for Flx15, Fig. 4). For seven repetitions of the 600-nm stimulus the ratio of the methyl-release rate at 3 min after delivery of the stimulus to the prestimulus rate was 0.79 ± 0.03 compared with 0.95 ± 0.05 for unstimulated cells (mean ± SEM). In *E. coli* the modulation of demethylation rate contributes to increases and decreases in transducer methylation that are responsible for adaptation to positive and negative stimuli, respectively. The behavioral effects of methylation inhibition in *H. halobium* (16, 21, 22), the phenotype of methylation mutants (16, 26), the results presented here, and the strong analogies with eubacterial chemotaxis, suggest the methylation system controls methyl-accepting transducers to cancel the effect of the receptor signals (i.e., receptor signal adaptation). The significance of the differences in kinetics of demethylation in *H. halobium* and *B. subtilis* compared with *E. coli* is not clear. In *B. subtilis* a posttransducer methyl-accepting component has been suggested to contribute a second source of methyl groups in this assay (36).

Background illumination of 600 nm generates a photostationary state mixture of SR-I$_{587}$ and its long-lived intermediate S$_{373}$, which is the repellent form of SR-I (4–6). Near-UV light (390 nm), at the intensities used here, excites S$_{373}$, generating a repellent response, and has negligible repellent effect through SR-II (Fig. 1). Transient methyl-release responses to the near-UV light occur in an orange (600 nm) background-dependent manner (Fig. 5), indicating an S$_{373}$-mediated effect (4–6). Small changes are seen in the absence of 600-nm background, which could be due to 2-photon cycling of SR-I or to a slight SR-II contribution. For S$_{373}$ as for SR-I$_{587}$ and SR-II, the reversal-inducing step change (in this case the step-up) causes a greater methyl-release response than the reversal-suppressing step change.

No methyl-release responses are observed in the retinal-deficient strain Flx5R in the absence of retinal, and both SR-I$_{587}$ and S$_{373}$-induced (but not SR-II-induced) methyl-release responses occur in this strain after addition of all-*trans*-retinal (data not shown).

The volatile methyl label released over the course of 30 min was 18% of that seen to be present on the taxis proteins from the same cell suspension determined by counting the bands from SDS/polyacrylamide gels, consistent with the decrease in total label over 30 min seen on the bands. Therefore, demethylation of the taxis proteins may account entirely for the volatile label in our measurements.

An Integrated Signal from SR-I and SR-II Regulates the Methylation System. SR-I in its attractant form and the repellent receptor SR-II have opposing effects on swimming behavior. When the two stimuli are delivered simultaneously,

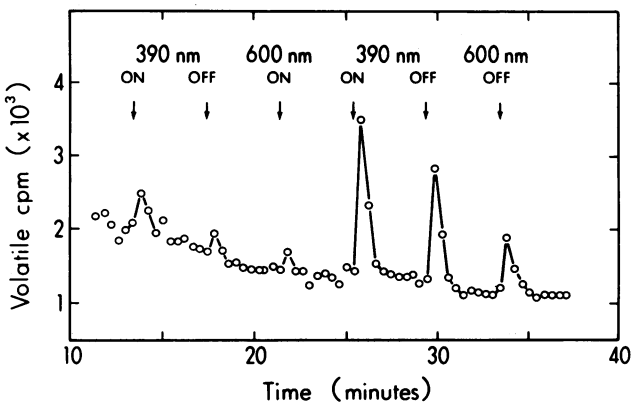

FIG. 5. Volatile [^{3}H]methyl release modulated by S$_{373}$. Assay conditions were as in Fig. 4. Strain was Flx15.

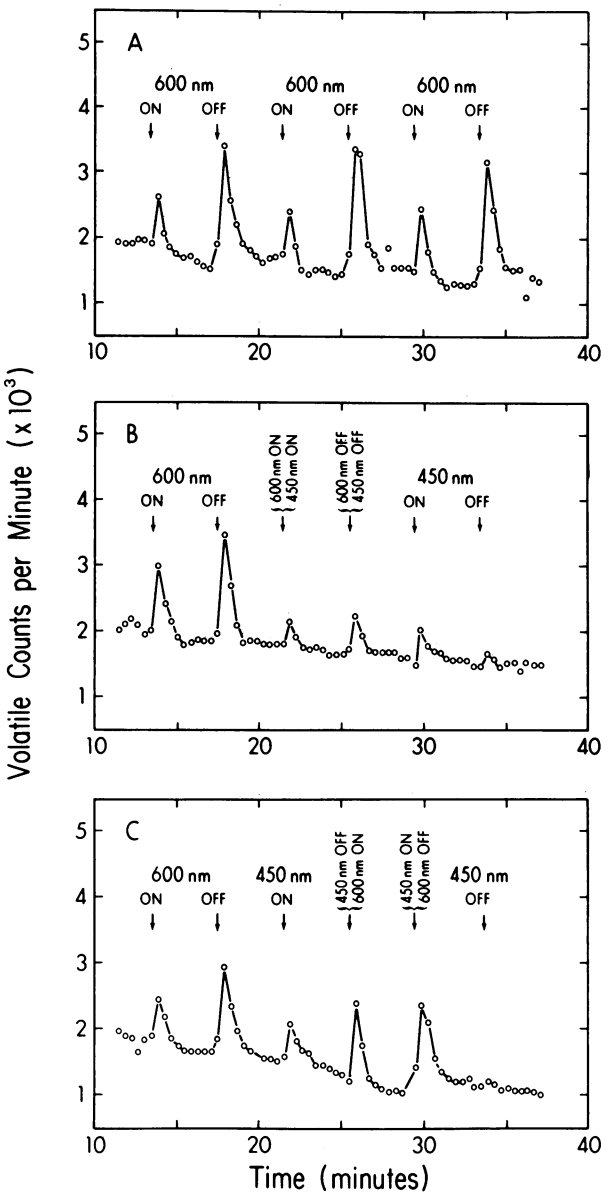

FIG. 6. Volatile [^{3}H]methyl release after simultaneous SR-I and SR-II stimuli. Assay conditions were as in Fig. 4. Strain was Flx15.

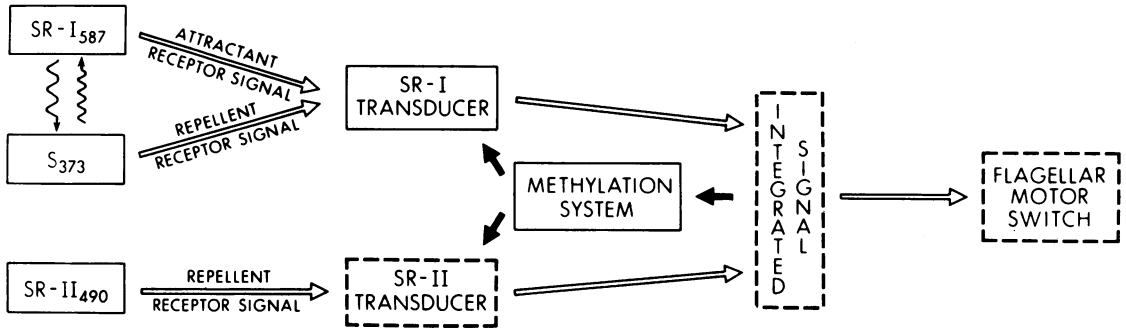

FIG. 7. Information transfer in the phototaxis signaling system of *H. halobium*. SR-I_{587} and S_{373} are the photoconvertible attractant and repellent forms of SR-I, and SR-II_{490} is a repellent receptor. Components detected biochemically are shown in solid boxes; dashed boxes indicate components the existence of which is supported by physiological studies.

the net behavioral effect results from an integrated signal from photoattractant and photorepellent receptor states (37, 38). Two opposing stimuli delivered through SR-I and SR-II simultaneously have a mutually canceling effect on methyl release, indicating the methylation system is regulated by an integrated signal from the two receptors (Fig. 6*B*). This hypothesis can be tested further by delivering reinforcing rather than opposing stimuli through the two receptors. A step-up in 600-nm light suppresses reversals through SR-I as does a step-down in 450 nm light through SR-II. Both of these reversal-suppressing stimuli delivered together produce a greater methyl release than either stimulus delivered alone (Fig. 6*C*). The same stimulus delivered repetitively with the temporal regime of this experiment produces reproducible responses over the period of the measurement (Fig. 6*A*).

Model of the Photosignaling Pathway. In Fig. 7, the SR-I chromoprotein is represented in its two photoconvertible states, the attractant form SR-I_{587} and the repellent form S_{373}, which exist in a photochromic equilibrium in visible light (4, 39). In the model, an attractant receptor signal is generated by photoconversion of SR-I_{587} into S_{373}, and a repellent signal by excitation of S_{373}, which returns the molecule to SR-I_{587} (through an intermediate state S^{b}_{510}). These receptor signals are likely to be photoinduced conformational states of the SR-I and SR-II chromoproteins that activate their transducers, most likely by protein–protein interaction. We propose two distinct transducers because photoactivation of SR-II modulates methylation in the absence of the intrinsic membrane protein of 94 kDa, the SR-I transducer according to our model. The transducers of SR-I and SR-II produce an integrated signal controlling the flagellar motor-switching probability (37, 38). The results above show the methylation system is also activated by an integrated signal from the receptors. We envision that the same integrated signal modulates both the switch and methylation system, as is the case in eubacteria (20).

We thank Wayne Hubbell and David Cincotta for the generous gift of [^{3}H]retinal, Wei-Dong Ding and Koji Nakanishi for help with the isomer purification, and Maqsudul Alam for a preprint of ref. 26. This research was supported by Public Health Service Grant GM27750 from the National Institutes of Health and Grant N-00014-89-j-1629 from the Office of Naval Research, both to J.L.S.

1. Spudich, J. L. & Bogomolni, R. A. (1988) *Annu. Rev. Biophys. Biophys. Chem.* **17**, 193–215.
2. Takahashi, T., Tomioka, H., Nakamori, Y., Tsujimoto, K., Kamo, N. & Kobatake, Y. (1988) in *Molecular Physiology of Retinal Proteins*, ed. Hara, T. (Yamada Science Foundation, Osaka, Japan), pp. 149–154.
3. Hildebrand, E. & Dencher, N. (1975) *Nature (London)* **257**, 46–48.
4. Spudich, J. L. & Bogomolni, R. A. (1984) *Nature (London)* **312**, 509–513.
5. Bogomolni, R. A. & Spudich, J. L. (1982) *Proc. Natl. Acad. Sci. USA* **79**, 6250–6254.
6. Takahashi, T., Mochizuki, Y., Kamo, N. & Kobatake, Y. (1985) *Biochem. Biophys. Res. Commun.* **127**, 99–105.
7. Dencher, N. A. & Hildebrand, E. (1979) *Z. Naturforsch.* **34**, 841–847.
8. Takahashi, T., Tomioka, H., Kamo, N. & Kobatake, Y. (1985) *FEMS Microbiol. Lett.* **28**, 161–164.
9. Wolff, E. K., Bogomolni, R. A., Scherrer, P., Hess, B. & Stoeckenius, W. (1986) *Proc. Natl. Acad. Sci. USA* **83**, 7272–7276.
10. Spudich, E. N., Sundberg, S. A., Manor, D. & Spudich, J. L. (1986) *Proteins* **1**, 239–246.
11. Marwan, W. & Oesterhelt, D. (1987) *J. Mol. Biol.* **195**, 333–342.
12. Tomioka, H., Takahashi, T., Kamo, N. & Kobatake, Y. (1986) *Biochem. Biophys. Res. Commun.* **139**, 389–395.
13. Spudich, E. N. & Spudich, J. L. (1982) *Proc. Natl. Acad. Sci. USA* **79**, 4308–4312.
14. Manor, D., Hasselbacher, C. A. & Spudich, J. L. (1988) *Biochemistry* **27**, 5843–5848.
15. Baryshev, V. A., Glagolev, A. N. & Skulachev, V. P. (1981) *Nature (London)* **292**, 338–340.
16. Spudich, E. N., Hasselbacher, C. A. & Spudich, J. L. (1988) *J. Bacteriol.* **170**, 4280–4285.
17. Springer, M. S., Goy, M. F. & Adler, J. (1979) *Nature (London)* **280**, 279–284.
18. Koshland, D. E., Jr. (1981) *Annu. Rev. Biochem.* **50**, 765–782.
19. Simon, M. I., Krikos, A., Mutoh, N. & Boyd, A. (1985) *Curr. Top. Membr. Transp.* **23**, 3–16.
20. Stewart, R. C., Russell, C. B., Roth, A. F. & Dahlquist, F. W. (1988) *Cold Spring Harbor Symp. Quant. Biol.* **53**, 27–40.
21. Schimz, A. & Hildebrand, E. (1979) *J. Bacteriol.* **140**, 749–753.
22. Spudich, J. L. & Stoeckenius, W. (1980) *Fed. Proc. Fed. Am. Soc. Exp. Biol.* **39**, 1972.
23. Schimz, A. (1981) *FEBS Lett.* **125**, 205–207.
24. Schimz, A. (1982) *FEBS Lett.* **139**, 283–286.
25. Bibikov, S. I., Baryshev, V. A. & Glagolev, A. N. (1982) *FEBS Lett.* **146**, 255–258.
26. Alam, M., Lebert, M., Oesterhelt, D. & Hazelbauer, G. L. (1989) *EMBO J.* **8**, 631–639.
27. Stock, J. B. & Koshland, D. E., Jr. (1978) *Proc. Natl. Acad. Sci. USA* **75**, 3659–3663.
28. Toews, M. I. & Adler, J. (1979) *J. Biol. Chem.* **254**, 1761–1764.
29. Kehry, M. R., Doak, T. G. & Dahlquist, F. W. (1984) *J. Biol. Chem.* **259**, 11828–11835.
30. Kehry, M. R., Doak, T. G. & Dahlquist, F. W. (1985) *J. Bacteriol.* **163**, 983–990.
31. Takahashi, T. & Kobatake, Y. (1982) *Cell Struct. Funct.* **7**, 183–192.
32. Sundberg, S. A., Alam, M. & Spudich, J. L. (1986) *Biophys. J.* **50**, 895–900.
33. Sundberg, S. A., Bogomolni, R. A. & Spudich, J. L. (1985) *J. Bacteriol.* **164**, 282–287.
34. Chelsky, D., Gutterson, N. I. & Koshland, D. E., Jr. (1984) *Anal. Biochem.* **141**, 143–148.
35. Schegk, E. S. & Oesterhelt, D. (1988) *EMBO J.* **7**, 2925–2933.
36. Thoelke, M. S., Kirby, J. R. & Ordal, G. W. (1989) *Biochemistry* **28**, 5585–5589.
37. Spudich, J. L. & Stoeckenius, W. (1979) *Photobiochem. Photobiophys.* **1**, 43–53.
38. Hildebrand, E. & Schimz, A. (1986) *J. Bacteriol.* **167**, 305–311.
39. Bogomolni, R. A. & Spudich, J. L. (1987) *Biophys. J.* **52**, 1071–1075.